

Application of μ -Synthesis based \mathcal{H}_∞ -Control for Adaptive Optics in Laser Material Processing

Steffen Mauch¹ and Johann Reger¹

Abstract—An adaptive optics system is used for the controlled attenuation of tip-tilt disturbances in an experimental laser material processing setup. It is shown that a \mathcal{H}_∞ -controller based on the μ -synthesis approach successfully accounts for the model uncertainties that, in the main, are unknown delays originating from the wavefront reconstruction and data transmission. The μ -synthesis problem is solved referring to a recently introduced non-smooth μ -optimization algorithm. Experimental results underscore the superiority of the presented approach in comparison to former results.

Index Terms—adaptive optics, robust control, \mathcal{H}_∞ -control, material processing, μ -synthesis

I. INTRODUCTION

As the costs for energy are increasing continuously, a lot of research is conducted on how to reduce the consumption of energy during product manufacturing processes. The economical goal here is that despite of increasing energy supply costs, the entire production costs shall decline or, at least, should remain constant.

In our research, we address the energy reduction problem as well as the increase of quality or accuracy in laser material processing. Amongst other issues, this means to cancel or reduce deteriorating effects on the wavefront which are due to thermal lenses and/or aberrations, see [1]. A correction of induced disturbances helps raise the local laser energy input into the workpiece and therefore renders possible smaller processing zones. This may yield better cutting or soldering results. Moreover, often the processing rate can be increased for processing the materials and therefore less energy per piece is necessary.

To this end, adaptive optics (short AO) are considered appropriate means for a real-time compensation of the disturbances on the wavefronts, not only in astronomy but also in laser material processing. First steps in the latter area have been conducted by *Fraunhofer Institute for Applied Optics and Precision Engineering (IOF)* in Jena/Germany where an experimental setup, including a deformable mirror was developed for increasing the beam quality in material processing with high power lasers. These technological achievements led us to employ a laboratory setup as depicted in Fig. 1. The wavefront is monitored by a shack-hartmann

wavefront sensor (WFS) and the WFS is connected to a real-time control system which calculates the wavefront so as to minimize the measured wavefront error and to compensate for the aberration. Naturally, the disturbance may be not measured directly because the effect of the tip-tilt and deformable mirror is always superposed.

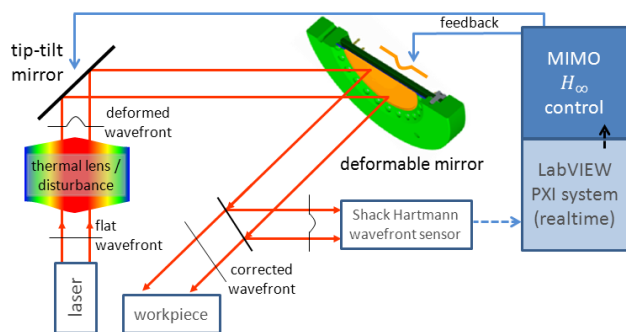


Fig. 1. Schematic diagram of the wavefront correction

Based on this wavefront correction setup we devise a μ -synthesis \mathcal{H}_∞ -controller for attenuating disturbances on the tip-tilt modes of the mirror. In our control application, we adhere to the μ -synthesis approach for maintaining a robust performance when subject to uncertainty. These uncertainties particularly originate from neglecting high frequency dynamics in the model, changes in assembly and adjustment variations, and from the data processing and transmission time-delay. Note that in the area of astronomy the \mathcal{H}_∞ -framework has already been applied within the control of deformable mirrors, see [2], [3], however, these approaches are neglecting time-delay, uncertainty within the system, and are theoretical contributions without an experimental validation.

The paper is organized as follows: Section II starts with more details on the experimental setup and the system model. In Section III, the control architecture as well as the used approach is explained circumstantially. The main contributions of the paper, e.g. the inclusion of not exactly known models and delay, are presented in Sections III and IV. Section IV contains a simulation study as well as experimental results. Section V is devoted to the conclusions and gives an outlook to some forthcoming works.

*The authors express their gratitude to Michael Appelfelder who is with the Institute of Applied Physics (IAP), Jena Univ., for his support. Thanks also to the German Federal Ministry of Education and Research (BMBF) and to the state of Thuringia in Germany for granting the excellence cluster *KD OptiMi2*.

¹All authors are with Control Engineering Group, Technische Universität Ilmenau, P.O. Box 10 05 65, D-98684, Ilmenau, Germany (e-mail: steffen.mauch@tu-ilmenau.de, reger@ieee.org)

II. EXPERIMENTAL PLANT MODEL

A. Experimental Setup

The experimental setup was already presented in [4]. It consists of a deformable mirror developed in-house by Fraunhofer IOF, a helium-neon laser, the tip-tilt mirror from PI (Physik Instrumente), a National Instruments LabVIEW PXI real-time system, and a shack-hartmann wavefront sensor. The shack-hartmann wavefront sensor (WFS) used is a HASO 3 Fast from Imagine Optic with CameraLink interface. The WFS is connected to a frame-grabber card which is installed in a performance computer. The WFS as well as the performance computer are capable to process about 905 frames per second.

As real-time system, the PXI-8110 is used which receives the slopes through gigabit ethernet. The performance computer is connected by gigabit ethernet to the real-time system and calculates the slopes out of the grabbed image. The system contains a delay of about 3–4 milliseconds arising due to data transfer over ethernet and slope calculations out of the image.

The tip-tilt mirror incorporates a built-in amplifier by default. Due to the mounting, the tip-tilt axis is rotated 45 degree with respect to the wavefront sensor. From there the coupling in the channels originate and the control problem is MIMO. Because the WFS is mounted on an adjusting platform the coupling is not exactly known.

The control algorithm is designed in MATLAB/Simulink, compiled via Simulink Coder and then included in the LabVIEW PXI system. For more detailed information on the experimental setup see [4].

B. Plant Model

The nominal model for the tip-tilt actuator was identified referring to measurements with a scanning vibrometer [4], i.e.

$$G_n(s) = \frac{514.9}{s^3 + 6432s^2 + 2.378e07s + 1.584e10}. \quad (1)$$

This model is subject to uncertainty due to the fact that during the identification process only frequencies until 1 kHz were used because the measurement is not as accurate in the high frequency as in the low frequency band (see Fig. 3 in [4]), and furthermore because there occurs a small, not very pronounced hysteresis that may therefore be approximated as time-invariant uncertainty. The nominal model is normalized to magnitude 1 since the reconstruction eliminates the different amplification, see [4].

The uncertainty may be captured by a transfer function that is gain bounded with

$$\|G_u\|_\infty \leq 0.1, \quad G_u \in \mathbb{R}(s). \quad (2)$$

We assume that the uncertainty is additive such that

$$G(s) = G_n(s) + G_u(s) \quad (3)$$

where $G(s)$ is the resulting uncertain transfer function. The assumption of an additive uncertainty is not considered

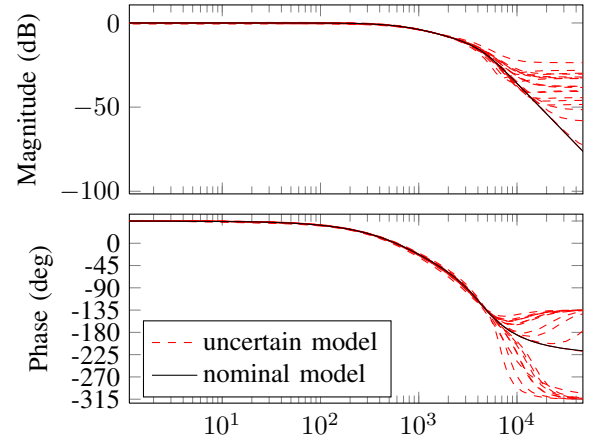


Fig. 2. Bode plot of the actuator with uncertainty

a restriction for instead it could also be reformulated as multiplicative uncertainty.

Since the wavefront measurement by camera is carried out on an adjustable platform there exists some rotational freedom that may result in uncertainty of the calculated slopes, too. This uncertainty also is modeled as an additive uncertainty with

$$\|\Delta_{\text{WFS}}\|_\infty \leq 0.05 \quad (4)$$

where $\Delta_{\text{WFS}} \in \mathbb{R}(s)^{2 \times 2}$.

Remark: As previously mentioned, the measuring axes of the WFS are rotated with respect to the axes of the tip-tilt mirror. In Fig. 3 this is symbolized by the block ‘WFS’. Its nominal behavior may be described by

$$\begin{pmatrix} x_{\text{WFS}} \\ y_{\text{WFS}} \end{pmatrix} = \underbrace{\sqrt{2} \begin{pmatrix} -0.5 & 0.5 \\ -0.5 & -0.5 \end{pmatrix}}_{\bar{G}_{\text{WFS}}} \begin{pmatrix} x_{\text{tip tilt}} \\ y_{\text{tip tilt}} \end{pmatrix} \quad (5)$$

which was validated by experiments and measurements. Therefore the overall transfer function reads

$$G_{\text{WFS}}(s) = \bar{G}_{\text{WFS}}(s) + \Delta_{\text{WFS}}(s). \quad (6)$$

Remark: An enhancement would be to model the hysteresis of the piezo actuators in the actuating mirrors, e.g. as a time-varying model uncertainty because piezo actuators may show pronounced hystereses resulting in a more complex synthesis problem, see e.g. [5], [6]. For the current application it turned out that improvement would be little.

III. CONTROL SETUP

In contrast to atmospheric turbulences, where many stochastic models exist for designing the AO systems, see [7], in laser material processing there is hardly any data available for modeling the occurring distortions. Thus in our case, instead of employing a classical \mathcal{H}_2 -control approach we opted for a μ -synthesis based \mathcal{H}_∞ -controller, as exposed in [8]–[10].

Within this framework and in view of the control-loop structure, depicted in Fig. 3, we are aiming at finding a

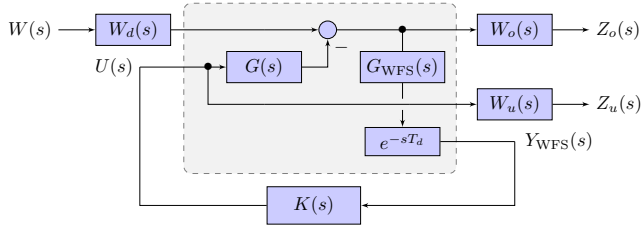


Fig. 3. Block diagram of the nominal control loop

controller $K(s)$ such that the \mathcal{H}_∞ norm of the transfer functions from $W(s)$ to $Z_o(s)$ and $Z_u(s)$ are minimized. Introducing the transfer functions via $Z_o(s) = S_{z_o w}W(s)$ and $Z_u(s) = S_{z_u w}W(s)$ the problem to be solved reads

$$\min_{K(s)} \left\| \begin{array}{c} S_{z_o w} \\ S_{z_u w} \end{array} \right\|_\infty = \min_{K(s)} \sup_{\omega} \bar{\sigma} \left(\begin{array}{c} S_{z_o w}(j\omega) \\ S_{z_u w}(j\omega) \end{array} \right) \quad (7)$$

which is a so-called S/KS mixed-sensitivity optimization problem, see [8]. The mixed-sensitivity approach allows for incorporating the limited bandwidth of the tip/tilt mirror and admits an improved disturbance rejection at the output. As is conventional, we are content with obtaining a suboptimal \mathcal{H}_∞ -controller that meets an upper bound on the \mathcal{H}_∞ norm.

A. Brief μ -Synthesis Review

The uncertainties in $G(s)$ and $G_{WFS}(s)$, introduced in (3) and (6), are handled in the robust control paradigm according to Fig. 4. The transfer function $T_{zw}(s)$ from $W(s)$ to $Z(s) = (Z_o(s), Z_u(s))^T$ results from

$$Z(s) = F_\ell \left(F_u(P(s), \Delta(s)), K(s) \right) W(s) = T_{zw}(s)W(s) \quad (8)$$

with F_ℓ and F_u denoting the lower and upper linear fractional transformations, respectively.

The goal of μ -synthesis here is to find a controller $K(s) \in \mathbb{R}(s)^{2 \times 2}$ such that when attached to the plant $P(s)$ the structured singular value μ with respect to transfer function $T_{zw}(s)$ and uncertainty $\Delta(s)$ is minimized, i.e. we minimize

$$\mu(\Delta, T_{zw}) = \frac{1}{\min \{ \bar{\sigma}(\Delta) : \det(I - T_{zw}\Delta) = 0 \}} \quad (9)$$

where $\bar{\sigma}(\Delta)$ is the maximum singular value of Δ . As a consequence, whenever

$$\bar{\sigma}(\Delta)\mu(\Delta, T_{zw}) < 1 \quad \forall s = j\omega \quad (10)$$

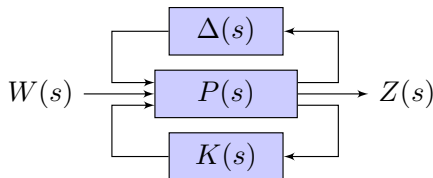


Fig. 4. Block diagram regarding Fig. 3 with uncertainty

then due to the small gain theorem no uncertainty with $\|\Delta\|_\infty \leq 1$ may destabilize the closed-loop system, see [8].

For robustness, the general objective is to design a controller that minimizes an upper bound on μ for the closed-loop system. Minimizing solutions are known for some special cases, only. For a stepwise reduction of the upper bound on μ , the so-called D-K iteration may be used which involves the iterative solution of the standard \mathcal{H}_∞ -controller design problem. Note that $\|F_\ell(P, K)\|_\infty \leq 1$ implies the bound $\mu(F_\ell(P, K)) \leq 1$. With appropriate ‘D-scalings’ the upper bound on μ may even be further reduced such that with $\mu \leq \bar{\mu}$ we have

$$\bar{\mu} = \inf_{\substack{D \in \mathcal{D} \\ K(s) \text{ proper, stabilizing}}} \|DF_\ell(P, K)D^{-1}\|_\infty. \quad (11)$$

where matrices $D \in \mathcal{D}$ have the major property that they commute with Δ . For more details see [9].

The problem is convex in each of the variables D and $K(s)$ separately, but as a whole generally it is not convex. Therefore, iterations in the sense of (11) may converge to just a local minimum or, in particular cases, the algorithm might not even converge. It is well-known that due to the biconvex nature of the D-K iteration and due to the pointwise computed D-scalings for selected frequencies (yielding no state space realization), in practice, major problems may arise, see [11].

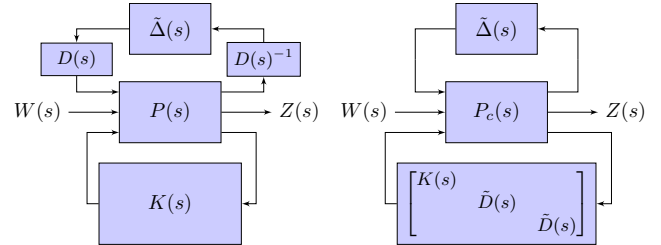


Fig. 5. Loop equivalence for D-scaling transformation

In some cases, these difficulties may be circumvented using the approach proposed in [11] where the order and the structure of the controller as well as the order of the D-scalings are chosen a priori. The corresponding fixed order \mathcal{H}_∞ -controller may be directly synthesized, see [12]. The algorithm has the advantage that a posteriori order reduction are not necessary. The obtained controller is not necessarily the optimal one due to the non-smoothness of the problem, thus, the achieved optimum could also be local. However, the robustness against uncertainties as well as the performance will not be affected by the typical controller reduction.

In order to take uncertainties into account, the approach may be combined with a μ -synthesis approach. The solution of the synthesis problem involves non-smooth optimization techniques. Using the transformations $\tilde{D}(s) = D(s) - I_N$, $\tilde{\Delta}(s) = D(s)^{-1}\Delta(s)D(s)$ and $\|\tilde{\Delta}\|_\infty \leq 1$, illustrated in

Fig. 5, we obtain

$$D_\omega F_\ell(P(j\omega), K(j\omega)) D_\omega^{-1} = F_\ell \left(P_c(j\omega), \begin{pmatrix} K(j\omega) & 0 & 0 \\ 0 & \tilde{D}(j\omega) & 0 \\ 0 & 0 & \tilde{D}(j\omega) \end{pmatrix} \right) \quad (12)$$

the \mathcal{H}_∞ norm of which has to be minimized along the same line as in (11) for all $\tilde{D}(s)$, and proper and stabilizing $K(s)$. For details see [11].

Remark: Some extensions also consider the handling of time-varying structured perturbations/uncertainties. For this case, necessary and sufficient conditions are given in [6].

B. Delay Handling

The system shows a non-negligible unknown delay which is upper and lower bounded. The delay results from an internal, fixed delay in the WFS due to the image processing and spot calculation. The fact that the delay is not exactly known results from the fact that the WFS is not triggered and, hence, not synchronized with the real-time system. Determination of the fixed delay is difficult due to that the trigger input from the WFS is not accurate. Since the real-time system does not operate with multiples of the frame rate of the WFS, one may argue that the delay is slowly time-varying. However, matching with the experiments it turns out that this effect is small, thus we assume a constant norm-bounded delay τ . In the denotation from above, hence

$$Y_{\text{WFS}}(s) = e^{-\tau s} G_{\text{WFS}}(s) Y(s). \quad (13)$$

Since the exponential is irrational, standard methods as e.g. the D-K iteration, may not be used since they require rational transfer functions. Therefore, as a simple choice we resort to the (rational) Padé-approximation of the delay

$$e^{-\tau s} \approx \frac{1 - k_1 s + k_2 s^2 + \dots + (-1)^n k_n s^n}{1 + k_1 s + k_2 s^2 + \dots + k_n s^n}$$

where n is the approximation order to be chosen. The coefficients k_i depend on n and τ and are determined from the fact that the Padé-approximation results from a Taylor series expansion of the transcendental function. In this case, a simple approximation with a first order delay is not sufficient because in the significant frequency band the deviation would be too large.

Since there is a lower and an upper bound on the delay and as it is assumed that it does not vary with time, it is now possible to handle the uncertain delay by an uncertain parameter.

For $n = 3$ the Padé-approximation reads

$$e^{-\tau s} \approx \frac{1 - \frac{\tau}{2}s + \frac{\tau^2}{10}s^2 - \frac{\tau^3}{120}s^3}{1 + \frac{\tau}{2}s + \frac{\tau^2}{10}s^2 + \frac{\tau^3}{120}s^3}$$

where τ is uncertain within $3 \text{ msec} \leq \tau \leq 4 \text{ msec}$ here¹. Fig. 6 shows phase plots for different uncertain parameters τ in

¹In contrast to [4], after due consideration of the missing synchronization and further measurements it turned out that the WFS shows a delay larger than 3 msec.

the frequency band of interest. The improvement of treating τ as uncertain is that the control loop is robustified against delay uncertainty, however, has a small impact on the loop performance.

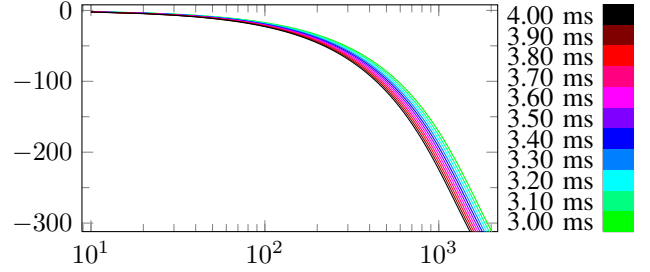


Fig. 6. Phase plot of the Padé-approximation for various τ

Applying the Padé-approximation, a suboptimal \mathcal{H}_∞ -controller respecting the time delay may now be calculated. However, the resulting controller has the same order as the extended plant. The orders of Padé-approximation, actuator model, and weighting functions all sum up to a controller order of far above 10. In case of $n = 3$, the overall plant and thus the controller is of order 18.

Remark: The uncertain real parameter τ is estimated as a complex uncertainty. This may be conservative, but helps simplify the synthesis. A less conservative alternative would be the ‘mixed μ -synthesis with multipliers’ approach. But this was not necessary for our purposes.

C. Controller Structure

The full order μ -synthesis \mathcal{H}_∞ -controller turns out to be too large to be successfully implemented on the real-time system. In light of this, one may apply order reduction techniques on the controller, e.g. balanced truncation via square root method, balanced stochastic model truncation (BST) via Schur method, to name but a few.

However, since the μ -synthesis of \mathcal{H}_∞ -controller with the D-K or D-G/K iteration² was not successful with the *dksyn* command from the ‘Robust Control Toolbox’ of Matlab, we followed the afore-mentioned approach presented in [11]. Hence, we chose the order and structure of the controller directly and synthesize a fixed order \mathcal{H}_∞ -controller. With the non-smooth μ -synthesis proposed in [11] and the Matlab command *hinfstruct* a state-space controller of order eight is calculated as a desired order \mathcal{H}_∞ -controller³. This order meets the capabilities of the real-time system.

Remark: The resulting controller has no integral action, as usual for \mathcal{H}_∞ -controllers. In cases when, other than here, steady state error is an issue—plant has no integral action—approaches as in [8] may be employed.

²For extending the D-K iteration to uncertain real parameters instead of complex ones see [8, chapter 18.2]

³Valuable hints for the correct formulation and solving of the problem within Matlab may be found in [13]

D. Weighting Functions

For imposing some frequency specifications on the control loop, weighting transfer functions have to be chosen that enter the loop structure as shown in Fig. 3. These are

$$W_d(s) = \frac{1}{0.1s + 1} \quad (14)$$

$$W_o(s) = 80 \frac{10s + 1}{(100s + 1)(0.001s + 1)} \quad (15)$$

$$W_u(s) = 0.6 \frac{0.05s + 1}{0.0003s + 1} \quad (16)$$

as depicted in Fig. 7. Weighting function $W_u(s)$ is chosen such that the constraints from the real-time system match with the actuator dynamics, but also takes into consideration actuation bounds. $W_d(s)$ is weighting the incoming disturbance where we respect that most disturbances are in the range up to 10 Hz. $W_o(s)$ is weighting the control deviation with an approximate integral behavior in the low frequency band for reduction of the stationary control deviation. A deviation in the higher frequency range is fined less so as to consider the limiting sampling time of the real-time system.

E. Resulting Controller

In our case, the resulting controller is specified to be of order eight. It has the state space representation:

$$K(s) = C(sI - A)^{-1}B + D$$

where

$$A = \begin{pmatrix} -0.74 & -8.03 & 0 & 0 & 0 & 0 & 0 & 0 \\ -1.02 & -10.1 & -0.636 & 0 & 0 & 0 & 0 & 0 \\ 0 & -4.74 & -9.13 & -7.83 & 0 & 0 & 0 & 0 \\ 0 & 0 & -7.72 & -3.28 & 1.75 & 0 & 0 & 0 \\ 0 & 0 & 0 & 4.68 & -4.87 & -2.02 & 0 & 0 \\ 0 & 0 & 0 & 0 & -2.77 & -6.73 & 0.82 & 0 \\ 0 & 0 & 0 & 0 & 0 & 2.25 & -10.1 & 6.95 \\ 0 & 0 & 0 & 0 & 0 & 0 & -4.49 & 2.86 \end{pmatrix}$$

$$B = \begin{pmatrix} -13.3 & 3.15 \\ -1.15 & -1.38 \\ 10.2 & -3.86 \\ -3.44 & 3.05 \\ 2.64 & -4.91 \\ -12.5 & 15.7 \\ 6.96 & -1.60 \\ 6.08 & -1.85 \end{pmatrix} \quad D = \begin{pmatrix} -0.274 & 0.00933 \\ 0.00494 & -0.271 \end{pmatrix}$$

$$C = \begin{pmatrix} 10.4 & -32.4 & -15.5 & 10.6 & -11.7 & -13.9 & -11.9 & 16.7 \\ 6.41 & -13.9 & -18.1 & 5.19 & -3.83 & -15.3 & -3.96 & 5.15 \end{pmatrix}$$

IV. SIMULATIONS AND EXPERIMENTS

A. Simulations

In the synthesis of the controller, the system performance was included by choosing the weighting functions accordingly. However, some parts were neglected as e.g. the fact that the experimental setup shows a sampling time of $T_s = 0.75$ msec and that the wavefront sensor is able to deliver 905 frames per second, only. Therefore, the controller shows a quite low dynamics such that an approximation incurs hardly any performance loss. In this regard, the conversion from continuous-time to discrete-time is done via the bilinear transform with $T_s = 0.75$ msec. For verifying the effects of the bilinear transformation and also of the Padé-approximation, simulations with noisy signals were carried out within Simulink. The outcome was that these effects may be well covered with the presented model. Fig. 8 and 9

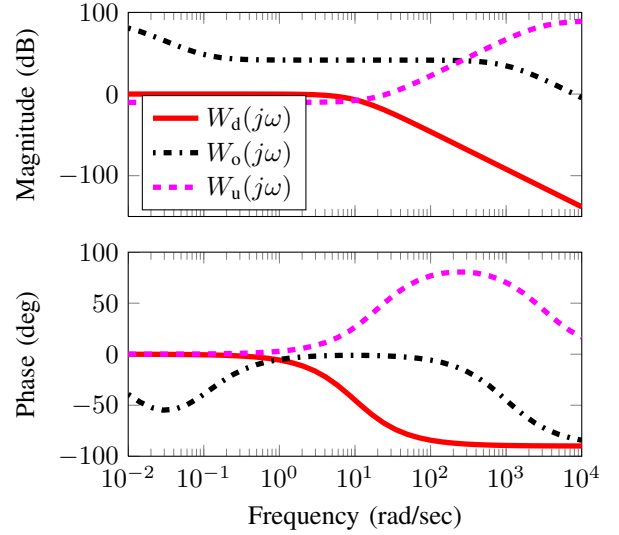


Fig. 7. Bode plot of the weighting functions

contain the bode plot and respective step response without these effects.

The bode plot of $S_{zow}(j\omega)$ in Fig. 8 indicates a cut-off frequency of about 100 Hz. Moreover, it is visible that the uncertainties do not much affect the performance. Simulation

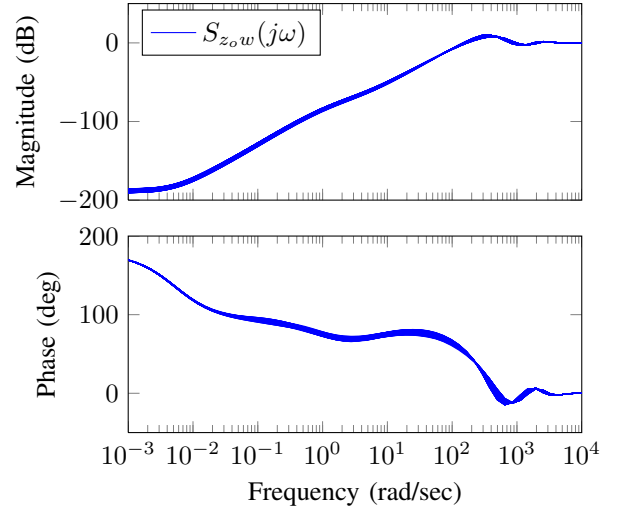


Fig. 8. Bode plot for 200 random uncertainties

results in Fig. 9 clearly visualize that although uncertainties and uncertain time-delay are present, the step response of the system does not change significantly. The controller impressively minimizes the influence of the uncertainties regardless of their source, i.e. from time-delay or uncertainty of the model. After about 12-16 msec the effect of the disturbance on the output has vanished. The swing-up at the beginning of the step-response is an effect of the Padé-approximation used for modeling the delay. The gray dashed line marks the 5% control deviation. Fig. 10 contains results of the simulation with a fixed time-delay of 3 msec and an implementation as

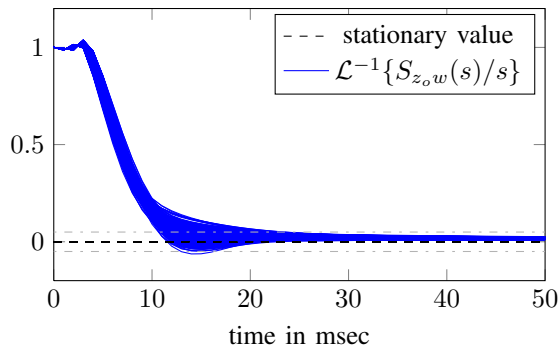


Fig. 9. Step response for 200 random uncertainties

zero order hold of $\frac{1}{905}$ sec. When comparing Fig. 9 and 10 one may notice a small deviation in the overshoot. The black line marks the time where disturbances (steps) have occurred during simulation. Finally, a comparison of Fig. 10 with the

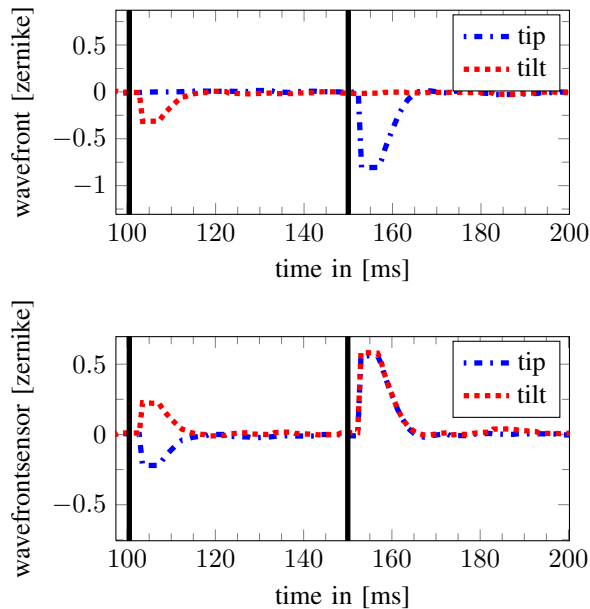


Fig. 10. Simulation results ($\tau = 3$ msec and noise)

simulation results presented [4] (see Fig. 11 for convenience) show a remarkable improvement in the overall performance.

B. Experiments

The experimental setup is equivalent to the setup in [4], where a PI-controller with Kalman-Filter as a disturbance observer was used. The discretized controller is compiled via the Simulink Coder and included in the PXI system as DLL.

Fig. 12 recalls the former experimental results with the PI-approach where uncertainties were neglected. With the PI-approach it takes about 20 msec to eliminate the disturbance whereas with the underlying \mathcal{H}_∞ -approach it takes only 12-16 msec, see Fig. 13 for the new experimental results. The former results compared with the new approach shown

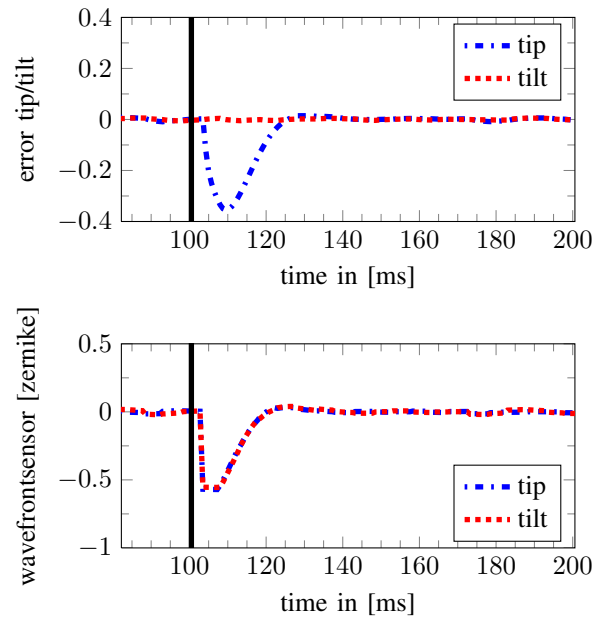


Fig. 11. Former simulation results based on PI-approach, see [4]

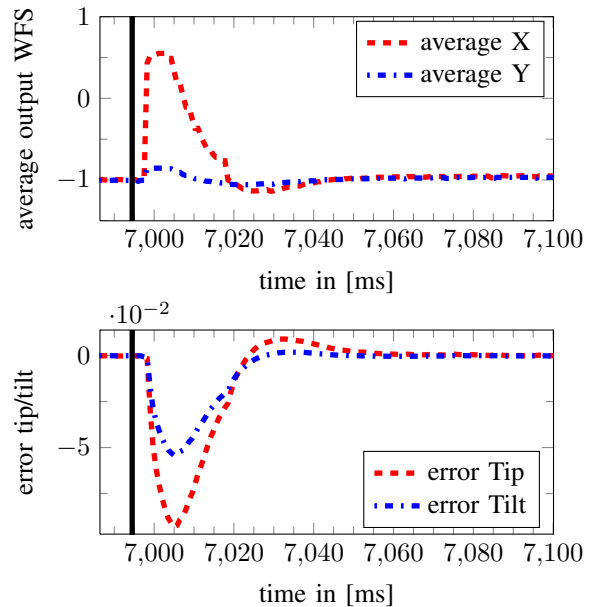


Fig. 12. Former experimental results with PI-approach, see [4]

in Fig. 13 shows a major improvement in the performance even when subject to uncertainty in the plant. E.g. the small overshoot in Fig. 12 has also been reduced with the new approach whereas the settling time has distinctly been shortened, see Fig. 13. The black line again marks the time instant when the disturbance has occurred. The figures underscore that not only in simulation results, but also in the experiments the performance of the new approach is superior to the former PI-approach in [4].

V. CONCLUSIONS

An application of a μ -synthesis based \mathcal{H}_∞ -controller design is presented that is able to attenuate disturbances in the presence of norm bounded uncertainties as well as delays within an adaptive optics system. The delay is not exactly known and uncertain, but assumed to be constant during the process. A novel approach from [11] has been used for solving the μ -synthesis problem since the usually employed D-(G)K iteration did not converge.

The resulting closed-loop performance was compared in simulations with the performance of the former approach, published in [4] which was not taking uncertainty into account. The controller was robustified against uncertainties as well as unknown delay, leaving the performance remarkably unaffected. This is a major advancement for the use in a real-world product which always will need to guarantee both robust stability and performance.

In further work, the control of higher order Zernike modes in the deformable mirror will receive a deeper attention. In this case, also the effects of time-varying delays might have to be reviewed. A first treatment may be referring to Rem. III-A or to the LMI approaches in [14], [15].

REFERENCES

- [1] J. D. Mansell, J. Hennawi, E. K. Gustafson, M. M. Fejer, R. L. Byer, D. Cluble, S. Yoshida, and D. H. Reitze, "Evaluating the Effect of Transmissive Optic Thermal Lensing on Laser Beam Quality With a Shack-Hartmann Wave-Front Sensor," *Appl. Opt.*, vol. 40, no. 3, pp. 366–374, Jan 2001.
- [2] M. Nagashima and B. Agrawal, "Active control of adaptive optics system in a large segmented mirror telescope," *International Journal of Systems Science*, pp. 1–17, 2012.
- [3] F. G. L. Baudouin, C. Prieur and D. Arzelier, "Control of adaptive optics system: an H-infinity approach," *IFAC World Congress on Automatic Control, Seoul, Korea, 2008*.

- [4] S. Mauch, J. Reger, and E. Beckert, "Adaptive Optics control for laser material processing," *Congreso Latinoamericano de Control Automático (CLCA 2012)*, 2012. [Online]. Available: <http://www.clca2012-papers.com/data/papers/10249.pdf>
- [5] N. Chuang and I. R. Petersen, "Robust H Infinity Control of Hysteresis in a Piezoelectric Stack Actuator," *IFAC 17th World Congress*, 2008.
- [6] K. Poola and A. Tikku, "Robust performance against time-varying structured perturbations," *Automatic Control, IEEE Transactions on*, vol. 40, no. 9, pp. 1589–1602, sep 1995.
- [7] J. W. Hardy, *Adaptive Optics for Astronomical Telescopes*. Oxford Series in Optical & Imaging Sciences, 1998.
- [8] K. Zhou and J. C. Doyle, *Essentials of Robust Control*, 1st ed. Prentice Hall, 10 1997.
- [9] K. Zhou, J. C. Doyle, and K. Glover, *Robust and Optimal Control*, 1st ed. Prentice Hall, 8 1995.
- [10] S. Skogestad and I. Postlethwaite, *Multivariable Feedback Control: Analysis and Design*, 2nd ed. Wiley-Interscience, 11 2005.
- [11] P. Apkarian, "Nonsmooth μ -synthesis," *International Journal of Robust and Nonlinear Control*, vol. 21(8), pp. 1493–1508, 2011.
- [12] P. Gahinet and P. Apkarian, "Structured h_∞ synthesis in matlab," *18th IFAC World Congress*, 2011.
- [13] P. Apkarian. (2012, Sept.) Examples for nonsmooth μ synthesis with Matlab. [Online]. Available: <http://pierre.apkarian.free.fr/>
- [14] K. Gu, V. L. Kharitonov, and J. Chen, *Stability of Time-Delay Systems*, 1st ed. Birkhuser Boston, 6 2003.
- [15] E.-K. Boukas and Z.-K. Liu, *Deterministic and Stochastic Time-Delay Systems*, 1st ed. Birkhäuser Boston, 3 2002.

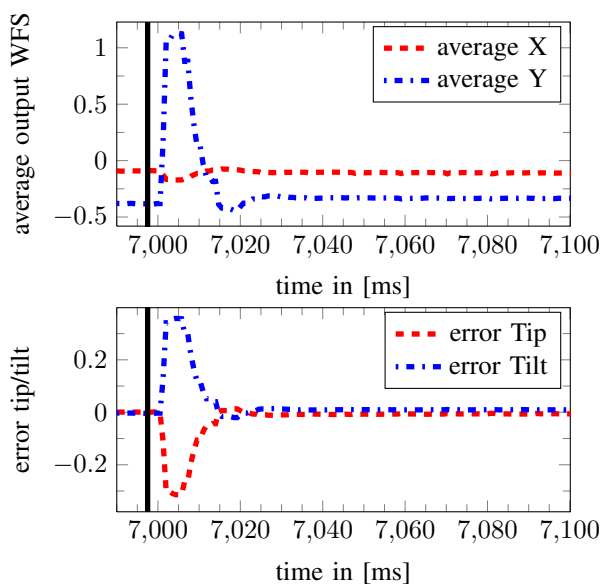


Fig. 13. Experimental results based on new controller